

The Millennium Galaxy Catalogue: The local supermassive black hole mass function in early- and late-type galaxies

Alister W. Graham^{1*}, Simon P. Driver², Paul D. Allen^{1,2} and Jochen Liske³

¹Centre for Astrophysics and Supercomputing, Swinburne University of Technology, Hawthorn, Victoria 3122, Australia

²SUPA†, School of Physics & Astronomy, University of St Andrews, North Haugh, St Andrews, Fife, KY16 9SS, UK

³European Southern Observatory, Karl-Schwarzschild-Str. 2, 85748 Garching, Germany.

Received 2006 Jan 01; Accepted 2006 December 31

ABSTRACT

We provide a new estimate of the local supermassive black hole mass function using (i) the empirical relation between supermassive black hole mass and the Sérsic index of the host spheroidal stellar system and (ii) the measured (spheroid) Sérsic indices drawn from 10k galaxies in the Millennium Galaxy Catalogue. The observational simplicity of our approach, and the direct measurements of the black hole predictor quantity, i.e. the Sérsic index, for both elliptical galaxies and the bulges of disc galaxies makes it straightforward to estimate accurate black hole masses in early- and late-type galaxies alike. We have parameterised the supermassive black hole mass function with a Schechter function and find, at the low-mass end, a logarithmic slope $(1 + \alpha)$ of ~ 0.7 for the full galaxy sample and ~ 1.0 for the early-type galaxy sample. Considering spheroidal stellar systems brighter than $M_B = -18$ mag, and integrating down to black hole masses of $10^6 M_\odot$, we find that the local mass density of supermassive black holes in early-type galaxies $\rho_{\text{bh,early-type}} = (3.5 \pm 1.2) \times 10^5 h_{70}^3 M_\odot \text{Mpc}^{-3}$, and in late-type galaxies $\rho_{\text{bh,late-type}} = (1.0 \pm 0.5) \times 10^5 h_{70}^3 M_\odot \text{Mpc}^{-3}$. The uncertainties are derived from Monte Carlo simulations which include uncertainties in the $M_{\text{bh}}-n$ relation, the catalogue of Sérsic indices, the galaxy weights and Malmquist bias. The combined, cosmological, supermassive black hole mass density is thus $\Omega_{\text{bh,total}} = (3.2 \pm 1.2) \times 10^{-6} h_{70}$. That is, using a new and independent method, we conclude that $(0.007 \pm 0.003) h_{70}^3$ per cent of the universe’s baryons are presently locked up in supermassive black holes at the centres of galaxies.

Key words: black hole physics — galaxies: bulges — galaxies: fundamental parameters — galaxies: luminosity function, mass function — galaxies: structure — surveys

1 INTRODUCTION

Two purely photometric properties of galaxies, or rather their spheroidal¹ components, are known to correlate strongly with a galaxy’s supermassive black hole (SMBH) mass M_{bh} . The first property is optical luminosity (Kormendy 1993; Franceschini et al. 1998; Magorrian et al. 1998). Due to the observation that SMBHs are associated with the ‘bulge’ of a galaxy, and not the disc, it is necessary to perform a bulge/disc decomposition if one is to properly treat lenticular and late-type galaxies. At present, apart from (Erwin, Graham & Caon 2002; their figure 3, with only eight

elliptical and five disc galaxies), no optically² calibrated relation that pertains to both elliptical galaxies and the bulges of disc galaxies is available. On the other hand, one can simply exclude the disc+bulge galaxies and only work with elliptical galaxies (e.g., McLure & Dunlop 2002, 2004).

In an effort to include disc galaxies, some authors have assigned some fixed fraction, such as three-tenths, of a disc galaxy’s total light to that of the bulge. However, given there is a known trend of decreasing bulge-to-total luminosity ratio with increasing morphological type (e.g., Hubble 1926, 1936; Kent 1985; Simien & de Vaucouleurs 1986; Andredakis, Peletier & Balcells 1995), the above approach introduces a systematic bias such that the SMBH masses

* AGraham@astro.swin.edu.au

† Scottish Universities Physics Alliance (SUPA)

¹ By the term ‘spheroidal’, we mean an entire elliptical galaxy or the dynamically hot component of a disc galaxy.

² A useful near-infrared $M_{\text{bh}}-L_{\text{spheroid}}$ relation is presented by Marconi & Hunt (2003), updated in Graham (2007).

are over-estimated in the late-type disc galaxies and under-estimated in the early-type disc galaxies, skewing the mid- to low-mass end of the SMBH mass function. Another approach has been to use the average bulge-to-total flux ratios derived from past $R^{1/4}$ -bulge + exponential-disc decompositions (Simien & de Vaucouleurs 1986). However, Andredakis & Sanders (1994) showed that Sb and Sc galaxies are, on average, better described with an exponential-bulge than an $R^{1/4}$ -bulge. Andredakis et al. (1995) subsequently showed that an $R^{1/n}$ -bulge was more appropriate, with the Sérsic index n shown to decrease with increasing disc galaxy type. While an $R^{1/4}$ -bulge plus exponential-disc results in an over-estimate of the B/D ratio when the bulge has a Sérsic index $n < 4$ (c.f. Figures 15 and 1 in Graham 2001), the use of an exponential-bulge + exponential-disc decomposition results in an under-estimate of the bulge-to-disc (B/D) flux ratio when the bulge actually possesses a Sérsic profile with $n > 1$ (Graham 2001, his figure 13). Therefore, $R^{1/n}$ -bulge plus exponential-disc fits are required. The various $M_{\text{bh}}-L$ relations in the literature predict SMBH masses that differ by factors of two to ten depending on the luminosity. This obviously inhibits the use of the $M_{\text{bh}}-L$ relation at present. An investigation of this problem is not undertaken here but presented in Graham (2007).

The second³ photometric quantity known to correlate with M_{bh} is the concentration of the stars in the host spheroidal stellar system (Graham et al. 2001, 2003). This concentration is monotonically related to the shape, i.e. the Sérsic index n , of the spheroid's light-profile (Trujillo, Graham & Caon 2001, their equation 6). Moreover, the $M_{\text{bh}}-n$ relation is known to be as tightly correlated as the $M_{\text{bh}}-\sigma$ relation and have the same small degree of scatter (see Novak, Faber & Dekel 2005 for a recent comparison of these relations).

Using an expanded galaxy set (27 galaxies) with updated distances and black hole masses, Graham & Driver (2007a) have recently shown that the $M_{\text{bh}}-n$ relation (see Fig.1) is curved rather than linear. Fitting a quadratic equation, they obtained

$$\log(M_{\text{bh}}) = 7.98(\pm 0.09) + 3.70(\pm 0.46) \log(n/3) - 3.10(\pm 0.84)[\log(n/3)]^2, \quad (1)$$

with an intrinsic scatter $\epsilon_{\text{intrinsic}} = 0.18_{-0.06}^{+0.07}$ dex. The total absolute scatter in $\log M_{\text{bh}}$ is 0.31 dex, which compares favourably with the value of 0.34 dex from the $\log M_{\text{bh}}-\sigma$ data and relation in Tremaine et al. (2002). The parameter in front of the second order term in Eq.1 is inconsistent with a value of zero at the 99.99 per cent confidence level.

We have explored here whether the departure from a linear relation may have been driven by an increased and uneven scatter, i.e. outliers⁴, at the high-mass end of the $M_{\text{bh}}-n$ relation, or whether the curvature is inherent in the rest of the data set. In Fig.2 we show the results of fitting

a log-quadratic relation after the removal of the five highest mass data points from Fig.1. The coefficient in front of the quadratic term is again found to be inconsistent with a value of zero, this time at the 99 per cent level, and all three coefficients remain consistent, at the 1σ level, with the values given in Eq.1.

Support for the $M_{\text{bh}}-n$ relation stems from its application to galaxies not included in its construction. For example, De Francesco et al. (2007) have recently measured a Sérsic index $n = 4.1$ for NGC 3998, from which one would predict $\log(M_{\text{bh}}/M_{\odot}) = 8.43$, in perfect agreement with the mass they derived from a kinematical study of the nuclear gas. In another example, Guhathakurta et al. (2006, their Figure S2) report a Sérsic index $n = 2$ for M31, which has a SMBH mass equal to $3.5 \times 10^7 M_{\odot}$ (Ferrarese & Ford 2005) and is therefore also in good agreement with the data in Fig 1. Furthermore, for a sample of 11 narrow-line Seyfert galaxies (Ryan et al. 2007), the $M_{\text{bh}}-n$ relation predicts SMBH masses in agreement with those derived using the size of the broad line region and the continuum flux, and suggests a problem with the (M_{bh} -luminosity)-derived masses.

The $M_{\text{bh}}-n$ relation also implies a maximum mass to which SMBHs have formed. The broad turn-over seen in Fig.1 peaks at $n = 11.9$, where the predicted 1σ range of SMBH masses spans 0.8 to $3.8 \times 10^9 M_{\odot}$ (Graham & Driver 2007a, their Eq.8). In Graham & Driver (2005, their figure 1), one can see that for $n \geq 5$ there is not that much difference in profile shape, and hence there should not be much difference in SMBH mass for galaxies with $n \geq 5$. Above $n \sim 12$, increasing n to infinity has almost no effect on the profile shape, and hence the SMBH masses should all be the same. Some kind of asymptotic-like $M_{\text{bh}}-n$ function is therefore in some sense demanded by the form of the Sérsic $R^{1/n}$ model. At the high- n end of the distribution, we do not believe that galaxies with $n > 11.9$ have smaller SMBH masses than those with $n < 11.9$, and we note that the log-quadratic $M_{\text{bh}}-n$ relation (held fixed for $n > 11.9$) appears more logical than say a rising linear $M_{\text{bh}}-n$ relationship. In passing, we note that the highest SMBH mass which has been directly measured in a quasar using reverberation mapping is only $2.6 \times 10^9 M_{\odot}$ (S50836+71, Kaspi et al. 2007) and is thus consistent with our predicted upper $1-\sigma$ range. The second highest quasar SMBH mass is $0.9 \times 10^9 M_{\odot}$ (3C273).

In this paper we employ the $M_{\text{bh}}-n$ relation in Eq.1 to derive the SMBH mass function using data from the Millennium Galaxy Catalogue (MGC), which is described in Section 2. Preliminary results have been presented in Driver et al. (2006b, 2006c). Using the bulge-disc decompositions of the brightest 10^4 MGC galaxies (Allen et al. 2006), in Section 3 we construct the SMBH mass function. In Section 4 we compare our results with previous efforts to measure the SMBH mass density, $\rho_{\text{bh},0}$, using other means. A summary of our analysis is provided in Section 5.

Throughout this paper, unless specified otherwise, we use $\Omega_{\Lambda} = 0.7$, $\Omega_M = 0.3$ and $h_{70} = H_0/(70 \text{ km s}^{-1} \text{ Mpc}^{-1})$.

³ A third photometric quantity that has been *predicted* to correlate well with SMBH mass is the central stellar density of the host spheroid (Graham & Driver 2007a, their section 6).

⁴ As noted in Graham & Driver (2007a, their Section 3.3), there is reason to suspect that the highest SMBH mass, pertaining to NGC 4486, may have been overestimated, perhaps by a factor of 4.

2 THE MILLENNIUM GALAXY CATALOGUE, AND OUR SPHEROID SAMPLE

The MGC is a medium-deep ($B_{\text{MGC}} = 24$ mag)⁵ imaging survey of the nearby universe with a median seeing of $1.27''$ and it has 96.1 per cent complete (99.8 per cent for $B_{\text{MGC}} < 19.2$ mag) redshift information for the MGC-BRIGHT sample of 10,095 objects with $B_{\text{MGC}} < 20$ mag (Driver et al. 2005). The imaging data was acquired with the 2.5 m Isaac Newton Telescope which surveyed 37.5 square degrees⁶ in a 35 arcmin wide strip along the equatorial sky from $10h$ to $14h 50'$ (Liske et al. 2003). Each field was observed for 750 seconds through a Kitt Peak National Observatory B -band filter (4407 Å). The survey reaches a depth of $\mu_{\text{limit}} = 26$ mag arcsec⁻², with objects catalogued down to $B_{\text{MGC}} = 24$ mag. For comparison, the Sloan Digital Sky Survey Data Release 5 (Adelman-McCarthy et al. 2007) has a median (r -band) seeing of $1.4''$ and an effective exposure time of 54.1 seconds per band, leading to a g -band (4686 Å) magnitude limit of 22.2 mag (roughly on an AB system, and with $B - g$ roughly one-third of a mag, Blanton & Roweis 2007).

The MGC redshift information has come from a number of sources, as previously detailed in Driver et al. (2005, their Table 1). The median redshift is 0.12 and sample selection effects are well understood (Driver et al. 2005; Liske et al. 2006).

Allen et al. (2006) have performed an $R^{1/n}$ -bulge plus exponential-disc decomposition, using GIM2D (Marleau & Simard 1998; Simard et al. 2002), for all 10,095 objects. In addition to the best-fitting bulge Sérsic index n , GIM2D derives the (not necessarily symmetric) upper and lower uncertainty, δn , on the Sérsic index. In Fig.3 we show these uncertainties in n as a function of n . The distribution is such that 68 per cent of the galaxies have an error on n of less than ~ 20 per cent. Repeat observations, under different seeing conditions and on different chips of the wide-field camera, exist for 682 galaxies. Fig.15 in Allen et al. (2006) shows the ability of GIM2D to consistently recover the Sérsic index of the spheroid component. The mean offset and standard deviation in the quantity $\Delta \log n$ from repeat observations was reported there to be -0.002 and 0.132 dex, respectively. However, that distribution has longer tails than expected from a Gaussian. This is due to 11 per cent of the objects whose galaxy ‘type’ (see Allen et al. 2006) was in disagreement. Excluding these objects⁷, the half-width of the 68 percentile is 0.0729 dex, which corresponds to an 18 per cent mismatch in the value of n . This figure agrees well with the formal GIM2D error observed in Fig.3, and also with the 20 per cent uncertainty used in Graham & Driver (2007a) and commonly reported in the literature (e.g. MacArthur,

Courteau & Holtzman 2003). In this paper we adopted the GIM2D-derived values for both n and δn , as given in the catalogue ‘mgc_gim2d’ which is publicly available at the MGC website⁸.

From the 10,095 galaxies in the MGC with $B_{\text{MGC}} < 20$ mag, we restrict the sample to those 7,745 objects with $0.013 < z < 0.18$. Many of these are disc-only systems and therefore rejected as potential black hole hosts. In passing we note that, once the attenuating effects of dust have been dealt with, the MGC displays a uniformly flat distribution in $\cos(i)$, where i is the inclination of the disk, as one would expect for a uniformly distributed sample of galaxies (Driver et al. 2007b, their figure 5). We further refine our galaxy sample by imposing the requirement that both the bulges and the elliptical galaxies, collectively referred to as ‘spheroids’, have half-light radii greater than 0.333 arcsec (1 pixel) and that the bulge-to-total luminosity ratio (B/T) is greater than 0.01 (based on the lower values observed by Graham 2001, his figure 15). This helped avoid bright nuclear components such as star clusters that may have been fitted with the $R^{1/n}$ model in GIM2D. We also required that the absolute spheroid luminosity be brighter than -18 B -mag (discussed further in Section 3.2.4). Finally, we required that the galaxies core colour be red, such that $(u - r)_{\text{core}} > 2.00$ mag, denoting the transition in the colour bimodality for the MGC (Driver et al. 2006a). We refer to the red sample as ‘Sample 3’. However in Section 5.2 we show that the effect of including galaxies with blue cores (Sample 1 and 2) does not significantly alter our results on the SMBH mass density.

We additionally construct two mutually exclusive subsamples, which we label ‘early-types’ and ‘late-types’. The distinction is based on whether a galaxy’s B/T ratio is greater than or less than 0.4. Our choice of 0.4 is lower than values of 0.5 or 0.6 which have often been used in the past. Figure 4 shows the B/T ratio for $\sim 3k$ MGC galaxies brighter than $B_{\text{MGC}} = 19$ mag and which satisfy the above criteria and which have also been classified by eye into three morphological bins (Driver et al. 2006a): early-type galaxies (E/S0), early-type spiral galaxies (Sabc) and late-type spiral galaxies (Sd/Irr). If one was to use a cut at $B/T = 0.5$ or 0.6 to identify the early-type galaxies, then one would miss roughly half of them.

2.1 Colour correction

Before proceeding, we note that Eq. 1 was constructed in the R -band, while the MGC galaxies have been imaged in the B -band. The presence of radial, $B - R$ colour gradients (e.g., La Barbera et al. 2005, and references therein) may therefore result in different values for the Sérsic index n in the two bands.

In general, colour gradients are known to be fairly small in observations of local, early-type galaxies more luminous than ~ -17 B -mag (e.g., Peletier et al. 1990; Taylor et al. 2005, and references therein). The SDSS-VAGC (Blanton et al. 2005) has Sérsic indices in the $ugriz$ passbands in their low-redshift catalogue. Although these indices are somewhat

⁵ B_{MGC} is the Galactic extinction corrected, SExtractor (BEST, Vega) apparent magnitude (Liske et al. 2003).

⁶ The actual usable area of sky reduced to 30.88 square degrees after excluding the ‘bad’ regions (around bright stars, diffraction spikes, CCD defects, CCD gaps, CCD edges, vignetted corner, etc.).

⁷ The half-width of the 68 percentile of the full distribution (i.e., all 682 galaxies) is 0.108 dex, which translates to a 28 per cent mismatch in the value of n , slightly higher than the formal GIM2D (1σ) error. This means that ~ 11 per cent of the data may have a larger uncertainty than is assigned by GIM2D.

⁸ <http://www.eso.org/~jlsike/mgc/>

different to ours, in that they are derived from a single $R^{1/n}$ -galaxy model rather than an $R^{1/n}$ -bulge plus exponential-disc model, we should be able to get some insight from these data for the early-type galaxies, or at least the (disc-less) elliptical galaxies. An analysis of Fig.5, which shows the difference between the SDSS r - and g -band Sérsic index, reveals that the median value of $\log(n_r/n_g)$ for galaxies with $n_r > 2.0$ — i.e. predominantly the early-type galaxies — is only 0.003 dex (after removal of the few obvious outliers with absolute values greater than 0.3 dex). We therefore apply no correction to our B -band Sérsic indices of the early-type ($B/T > 0.4$) galaxies.

The single $R^{1/n}$ -galaxy models that have been applied to the SDSS data are not suitable for quantifying possible changes, with wavelength, to the Sérsic indices of bulges in late-type galaxies. Instead, we use the B - and R -band Sérsic indices from the bulges of 86 disc galaxies given by Graham (2003), 79 of which have indices in both bands. The average (\pm std.dev.) of the 79 values of $\log(n_R/n_B)$ is 0.09 (± 0.15). Splitting the sample into Sa–Sb and Sc–Sd–Sm galaxies gave the same small offset of 0.09 dex for each grouping. This suggests that the difference in n is not a function of spiral galaxy type nor bulge size. In addition to radial stellar population gradients across the bulges, a plausible contributor to this difference is dust. If the dust in spiral galaxies is more abundant at their centres, it will redden their centres more than their outskirts, reducing the central parts of the B -band light profile relative to the R -band light profile and thereby yielding smaller Sérsic indices for the bulge in the B -band. The similar B - and R -band Sérsic indices for the early-type galaxies suggests that dust is not a significant issue in these systems. MacArthur et al. (2003) also provide B - and R -band Sérsic indices for an independent sample of 47 and 43 late-type spiral galaxies, respectively — with 42 in common. In those instances where MacArthur et al. (2003) provided multiple Sérsic indices for the same galaxy in the same passband, we averaged the logarithm of the Sérsic indices. The average (\pm std.dev.) of the 42 values of $\log(n_R/n_B)$ is 0.08 (± 0.17), in good agreement with the data from Graham (2003). In deriving the SMBH mass function using Eq. 1 (established in the R -band), we will therefore apply a positive correction of 0.09 dex to the logarithm of the B -band Sérsic indices from the bulges of our MGC late-type galaxies.

The presence of two distinct populations in Fig.5, rather than one continuous distribution, suggests that the step-like correction we will apply to the Sérsic indices of our early- and late-type galaxies (0.0 dex and 0.09 dex respectively) may be more appropriate than a continuous correction based on some parameter such as the B/T ratio.

3 SMBH MASS FUNCTION AND SPACE DENSITY

To derive the SMBH mass function, we first modify the Sérsic indices of the late-type systems by 0.09 dex to convert from the B -band to the R -band, in accord with the previous Section. We then derive individual black hole masses for each spheroid using equation 1. For each black hole we determine an associated space-density weighting based on the MGC blue and red spheroid luminosity functions as derived

Table 1. Supermassive black hole mass function data (corrected for Malmquist bias) for the full, early- and late-type galaxy sample (Sample 3, see Section 5.2) shown in Fig. 6. The uncertainties given are the upper and lower quartiles (i.e. ± 25 per cent) from extensive Monte Carlo realisation of the combined errors.

$\log_{10} M_{\text{bh}}$ M_{\odot}	$\phi(10^{-4} h_{70}^3 \text{ Mpc}^{-3} \text{ dex}^{-1})$		
	All galaxies	Early-type	Late-type
5.00	0.42 ^{+0.13} _{-0.11}	0.11 ^{+0.08} _{-0.05}	0.34 ^{+0.11} _{-0.10}
5.25	0.00 ^{+0.13} _{-0.00}	0.21 ^{+0.08} _{-0.06}	0.00 ^{+0.11} _{-0.00}
5.50	0.00 ^{+0.16} _{-0.00}	0.00 ^{+0.10} _{-0.00}	0.02 ^{+0.12} _{-0.02}
5.75	0.55 ^{+0.17} _{-0.16}	0.31 ^{+0.11} _{-0.09}	0.25 ^{+0.12} _{-0.11}
6.00	1.29 ^{+0.20} _{-0.17}	0.19 ^{+0.16} _{-0.12}	1.13 ^{+0.13} _{-0.12}
6.25	0.00 ^{+0.27} _{-0.00}	0.00 ^{+0.28} _{-0.00}	0.00 ^{+0.13} _{-0.00}
6.50	0.76 ^{+0.51} _{-0.42}	0.37 ^{+0.47} _{-0.42}	0.37 ^{+0.14} _{-0.13}
6.75	3.23 ^{+0.54} _{-0.54}	2.48 ^{+0.51} _{-0.52}	0.73 ^{+0.14} _{-0.13}
7.00	4.97 ^{+0.54} _{-0.52}	4.61 ^{+0.54} _{-0.51}	0.36 ^{+0.15} _{-0.14}
7.25	6.58 ^{+0.59} _{-0.61}	6.06 ^{+0.58} _{-0.58}	0.53 ^{+0.16} _{-0.15}
7.50	6.40 ^{+0.72} _{-0.68}	6.02 ^{+0.67} _{-0.63}	0.36 ^{+0.17} _{-0.16}
7.75	9.45 ^{+1.15} _{-1.01}	8.31 ^{+1.03} _{-0.90}	1.15 ^{+0.21} _{-0.19}
8.00	16.29 ^{+1.74} _{-1.36}	15.55 ^{+1.54} _{-1.27}	0.71 ^{+0.26} _{-0.22}
8.25	20.06 ^{+2.26} _{-1.89}	17.56 ^{+1.79} _{-1.50}	2.56 ^{+0.56} _{-0.42}
8.50	16.79 ^{+1.85} _{-1.70}	13.02 ^{+1.57} _{-1.25}	3.73 ^{+0.49} _{-0.48}
8.75	7.53 ^{+2.13} _{-2.22}	5.81 ^{+1.75} _{-1.71}	1.78 ^{+0.45} _{-0.49}
9.00	3.26 ^{+1.41} _{-3.34}	1.96 ^{+1.31} _{-2.24}	1.47 ^{+0.33} _{-0.91}
9.25	0.00 ^{+1.88} _{-0.00}	0.00 ^{+1.13} _{-0.00}	0.00 ^{+0.67} _{-0.00}
9.50	0.00 ^{+0.16} _{-0.00}	0.00 ^{+0.03} _{-0.00}	0.00 ^{+0.12} _{-0.00}

Note: number densities are scaled to per unit $\log M_{\text{bh}}$ interval and not per 0.25 $\log M_{\text{bh}}$ interval.

in Driver et al. (2007a). The weight is the space density, $\phi(L)$, of the appropriate spheroid type (red or blue, divided at $(u-r)_{\text{core}} = 2.0$ mag) in the specified luminosity interval, L , divided by the number of galaxies which contributed to that interval, $N(L)$. The red and blue spheroid luminosity functions of Driver et al. (2007a) were derived via ‘vanilla’ step-wise maximum likelihood (see Efstathiou, Ellis & Peterson 1988) with K-corrections and e-corrections as defined in Driver et al. (2007a). The red and blue spheroid functions show markedly different forms and the justification for the segregation into two colour types is also given in Driver et al. (2007a).

The SMBH mass functions are then derived by summing the distribution of black hole mass times weights, i.e., $\phi(M_{\text{bh}}) = \sum W(L) M_{\text{bh}}$, where $W(L) = \phi(L)/N(L)$. This was constructed for black holes derived from all galaxies, early-types only ($B/T > 0.4$) and late-types only ($B/T \leq 0.4$). See Fig.6 for a graphic representations and Table 1 for a tabulated version of these distributions.

There are a number of sources of potential error. We model these via Monte Carlo simulations, following both individually and collectively the uncertainties on: the parameters defining equation 1; the Sérsic indices; the luminosity function weights; and the Malmquist bias⁹. Errors not modelled at this stage because they are considered secondary are uncertainties in the: K-corrections; e-corrections; dust attenuation; spectroscopic incompleteness; photometric errors effecting the magnitudes and hence weights; luminosity dependent cosmic variance; and the choice of colour cut in

⁹ Here we define Malmquist bias to be the systematic bias in our final measurements due to the presence of errors in our data.

the derived red and blue spheroid luminosity functions. Note that the global cosmic variance for the MGC survey area was derived in Driver et al. (2005) by comparison to mock catalogues produced by the Durham group¹⁰; this amounts to an overall uncertainty of 6 per cent in all $4 \times 10,001$ Monte Carlo simulations.

The Monte Carlo simulations consist of repeating the above analysis 10,001 times with the input values perturbed by the listed errors individually and collectively, i.e., $4 \times 10,001$ Monte Carlo simulations in all. All error distributions are assumed to be Gaussian. The impact of the error(s) is(are) then assessed by comparing the median and standard deviations of the derived distributions to the original estimate.

Table 2 summarises the cumulative sum of the SMBH mass functions, $\rho_{\text{bh},0}$, with error estimates from each of the above sources. In all cases we see that the dominant error is from the uncertainty in equation 1. This is perhaps not surprising since equation 1 is based on a quadratic fit to only 27 systems for which both credible black hole masses and Sérsic indices exist. Improvements in this method will therefore come from a larger calibration sample (similarly for the $M - \sigma$ and $M - L$ relations) and this should be attainable with next generation facilities. Perhaps surprising is that the errors in the Sérsic distribution have relatively little impact. In part this is indicative of the size of the sample but also helped by the quadratic nature of the $M - n$ relation preventing high n values leading to unreasonably large M_{bh} values. The errors from the luminosity function (i.e., statistics and cosmic variance) appear negligible, with cosmic variance the most significant.

Finally, we correct for the Malmquist bias in a rather straightforward manner. This is achieved by measuring $\rho_{\text{bh},0}$ assuming no errors and then remeasuring it but allowing all of the above errors to be perturbed simultaneously via Monte Carlo simulations. The difference between the two estimated values (raw and the median of the Monte Carlo simulations) provides a crude measurement of the systematic offset caused by the errors inherent in our data. To provide Malmquist bias corrected values we then subtract this systematic from our original values (~ 1 to 3 per cent downward correction). These final Malmquist bias corrected values are those shown in Tables 1 and 2.

Fig.6 shows the resulting black hole mass functions, where the error bars indicate the combined errors derived from the Monte Carlo analysis but excluding the cosmic variance error (as this is a hidden systematic and not a random error). Our resulting SMBH mass functions (and number density and mass density) depend on the Hubble constant. As was shown in Graham & Driver (2007a), the $M_{\text{bh}}-n$ relation is independent of the Hubble constant. This is because the Sérsic index n does not depend on galaxy distance, and while the SMBH mass does depend on distance, the overwhelming majority of galaxies that were used to construct the $M_{\text{bh}}-n$ relation had their distances obtained by Tonry et al. (2001) using surface brightness fluctuations — a technique that provides distances without assuming some Hubble constant. The mass function dependence on the Hubble constant arises from the $1/V_{\text{max}}$ weighting given

Table 2. The space density of matter in supermassive black holes. The errors are 1- σ values, after excluding 3- σ outliers. The densities given in Table 1, rather than the fitted empirical models, have been integrated down to SMBH masses of $10^6 M_{\odot}$. The final column shows the density normalised against the critical density. The reason why the density varies with h^3 and not h^2 is explained in Section 3. Factoring in the intrinsic scatter, Δ , from the $M_{\text{bh}}-n$ log-quadratic relation, the numbers in this Table should be increased by $\exp[(\Delta \ln 10)^2/2]$, which equals 1.09 if $\Delta = 0.18$ dex (Graham & Driver 2007a).

	No. Bulges	$\rho_{\text{bh},0}^a \pm \delta_1^b \pm \delta_2^c \pm \delta_3^d \pm \delta_4^e$ $h_{70}^3 10^5 M_{\odot} \text{ Mpc}^{-3}$	Ω_{bh} $10^{-6} h_{70}$
Early- and Late-type ($B/T > 0.01$)			
Sample 1	1769	$4.87 \pm 1.84 \pm 0.07 \pm 0.01 \pm 0.29$	3.6 ± 1.4
Sample 2	1676	$4.53 \pm 1.63 \pm 0.07 \pm 0.01 \pm 0.27$	3.3 ± 1.2
Sample 3	1543	$4.41 \pm 1.65 \pm 0.07 \pm 0.01 \pm 0.26$	3.2 ± 1.2
Early-type ($B/T > 0.4$)			
Sample 1	1539	$3.78 \pm 1.28 \pm 0.06 \pm 0.01 \pm 0.23$	2.8 ± 1.0
Sample 2	1485	$3.57 \pm 1.21 \pm 0.06 \pm 0.01 \pm 0.21$	2.6 ± 0.9
Sample 3	1352	$3.46 \pm 1.14 \pm 0.06 \pm 0.01 \pm 0.21$	2.5 ± 0.9
Late-type ($0.01 < B/T \leq 0.4$)			
Sample 1	230	$1.14 \pm 0.56 \pm 0.04 \pm 0.01 \pm 0.07$	0.8 ± 0.4
Sample 2	191	$0.95 \pm 0.49 \pm 0.03 \pm 0.01 \pm 0.06$	0.7 ± 0.4
Sample 3	191	as above	

^a Malmquist bias corrected.

^b Monte Carlo simulation of the errors in the $M_{\text{bh}}-n$ relation assuming a Gaussian error distribution.

^c Monte Carlo simulation of the error in n as specified by GIM2D and assuming a Gaussian error distribution.

^d Monte Carlo simulations of the error in the individual galaxy weights assuming a Gaussian error distribution.

^e MGC global cosmic variance of 6 per cent for the effective ~ 30 sq degree region with $0.013 < z < 0.18$.

to each galaxy; it is this volume term which introduces an h^3 dependence.

3.1 Parameterisation of the SMBH mass function

We have fitted two empirical models to our SMBH mass functions over the mass range $10^6 < M_{\text{bh}}/M_{\odot} < 10^9$. The first is a mild variation of the commonly-used 3-parameter Schechter (1976) function, and is given by

$$\phi(M_{\text{bh}}) = \phi_* \left(\frac{M_{\text{bh}}}{M_*} \right)^{\alpha+1} \exp \left[1 - \left(\frac{M_{\text{bh}}}{M_*} \right) \right], \quad (2)$$

where $\phi(M_*) = \phi_*$ (per unit $d \log(M_{\text{bh}})$ per Mpc^3). The turnover of the mass function and the maximum density occur at the SMBH mass

$$M_{\text{max}} = (\alpha + 1)M_*, \quad \alpha + 1 > 0 \quad (3)$$

where the associated maximum density is

$$\phi_{\text{max}} = \phi_* (\alpha + 1)^{\alpha+1} \exp[-\alpha]. \quad (4)$$

The logarithmic slope at the low-mass end of the mass function is given by the exponent $1 + \alpha$; a value of $\alpha = -1$ therefore corresponds to a flat distribution, and larger values correspond to a decreasing function as the SMBH mass decreases. For the early-type galaxy samples the slope ($1 + \alpha$) is ~ 1 (see Table 3). For the (early+late)-type samples the slope is approximately two-thirds; the shallower decline

¹⁰ <http://star-www.dur.ac.uk/~cole/mocks/>

is due to the contribution of SMBHs in late-type galaxies. These, and the other, best-fitting parameters are reported in Table 3 and the fits themselves are shown in Fig.6.

We explored the suitability of a second model having an additional fourth parameter such that the mass term in the exponential of equation 2 is raised to the power of β to give

$$\phi(M_{\text{bh}}) = \phi_* \left(\frac{M_{\text{bh}}}{M_*} \right)^{\alpha+1} \exp \left[1 - \left(\frac{M_{\text{bh}}}{M_*} \right)^\beta \right] \quad (5)$$

(Aller & Richstone, their equation 10). Our data, however, did not justify the need for this additional parameter. For the (early+late)-type samples, the value of β equalled 1.0 ± 0.1 . For the early-type sample, it ranged from 0.3 to 0.5, but did not give rise to significantly better fits. For this reason we do not show the fits or the parameters from this model. (Neither equations 2 nor 5 provided an acceptable description to the SMBH mass function in our late-type galaxy sample.)

3.2 Integrating the SMBH mass function

3.2.1 SMBH number density

The total SMBH number density can be obtained by integrating equation 2 with respect to $\log(M_{\text{bh}})$ (because ϕ is expressed in units of $h_{70}^3 \text{ Mpc}^{-3}$ per *decade* in SMBH mass). Integrating over $10^6 < M_{\text{bh}}/M_\odot < 10^9$, the number density is given by the expression

$$\begin{aligned} & \int_{\log(M_{\text{bh}}/M_\odot)=6}^{\log(M_{\text{bh}}/M_\odot)=9} \phi(M_{\text{bh}}) \, d \log M_{\text{bh}} \\ &= \int_{M_{\text{bh}}=10^6 M_\odot}^{M_{\text{bh}}=10^9 M_\odot} \frac{\phi(M_{\text{bh}})}{\ln(10) M_{\text{bh}}} \, dM_{\text{bh}} \\ &= \frac{\phi_* e^1}{\ln(10)} \left[\gamma \left(\alpha + 1, \frac{10^9 M_\odot}{M_*} \right) - \gamma \left(\alpha + 1, \frac{10^6 M_\odot}{M_*} \right) \right] \end{aligned} \quad (6)$$

where $\gamma(a, x)$ is the incomplete gamma function (e.g., Press et al. 1992) defined by

$$\gamma(a, x) = \int_0^x e^{-t} t^{a-1} dt. \quad (7)$$

For the early- and late-type galaxy values of ϕ_* , M_* and α (given in Table 3), the number density of SMBHs with masses between one million and one billion solar masses is $2.3 \times 10^{-3} h_{70}^3 \text{ Mpc}^{-3}$. For the early-type galaxies, the number density is $2.1 \times 10^{-3} h_{70}^3 \text{ Mpc}^{-3}$.

These values are an order of magnitude smaller than those reported in Shankar et al. (2004). The difference can be attributed to their rising ($M_{\text{bh}}-L$)-derived SMBH mass function (for all galaxy types) as one moves towards lower-masses. In contrast, our ($M_{\text{bh}}-n$)-derived mass function shows the opposite behaviour at the low-mass end.

3.2.2 SMBH mass density

In so far as equation 2 represents the mass function over the SMBH mass range $10^6 < M_{\text{bh}}/M_\odot < 10^9$, the SMBH mass

density for SMBHs having such masses can be obtained from

$$\begin{aligned} \rho_{\text{bh}} &= \int_{\log(M_{\text{bh}}/M_\odot)=6}^{\log(M_{\text{bh}}/M_\odot)=9} \phi(M_{\text{bh}}) M_{\text{bh}} \, d \log M_{\text{bh}} \\ &= \frac{\phi_* M_* e^1}{\ln(10)} \left[\gamma \left(\alpha + 2, \frac{10^9 M_\odot}{M_*} \right) - \gamma \left(\alpha + 2, \frac{10^6 M_\odot}{M_*} \right) \right]. \end{aligned} \quad (8)$$

Using the best-fitting parameters in Table 3, we obtain $\rho_{\text{bh}} = 4.3 \times 10^5 h_{70}^3 M_\odot \text{ Mpc}^{-3}$ (all-types), and $\rho_{\text{bh}} = 4.0 \times 10^5 h_{70}^3 M_\odot \text{ Mpc}^{-3}$ (early-types). Integrating the mass function over *all* masses increases the above values to $4.8 \times 10^5 h_{70}^3 M_\odot \text{ Mpc}^{-3}$ and $4.2 \times 10^5 h_{70}^3 M_\odot \text{ Mpc}^{-3}$, respectively.

We have, however, opted not to use the above formula, but to instead acquire the SMBH mass densities directly from our data, rather than from the fitted model.

Computing the local mass density, and integrating down to SMBH masses of $10^6 M_\odot$, we obtain $\rho_{\text{bh,early-type}} = (3.5 \pm 1.2) \times 10^5 h_{70}^3 M_\odot \text{ Mpc}^{-3}$ while $\rho_{\text{bh,late-type}} = (1.0 \pm 0.5) \times 10^5 h_{70}^3 M_\odot \text{ Mpc}^{-3}$. These results are presented in Table 2.

The above densities correspond to $\Omega_{\text{bh,early-type}} = \rho_{\text{bh,early-type}}/\rho_{\text{crit}} = (2.5 \pm 0.9) \times 10^{-6} h_{70}$, and $\Omega_{\text{bh,late-type}} = (0.7 \pm 0.4) \times 10^{-6} h_{70}$ (see Table 2), where $\rho_{\text{crit}} = 3H_0^2/8\pi G$ is the critical density for flat space¹¹. For reference, using an independent technique, Fukugita & Peebles (2004, their equation 75) give $2.5^{+2.5}_{-1.2} \times 10^{-6}$ for the SMBHs in early-type galaxies, and $1.3^{+1.2}_{-0.7} \times 10^{-6}$ for the SMBHs in late-type galaxies.

In deriving the (linear) SMBH mass density, $\rho_{\text{bh},0}$ (i.e., not $\log \rho_{\text{bh},0}$) from the convolution of the distribution function of n with the $\log M_{\text{bh}}-\log n$ relation, one needs to allow for the intrinsic scatter in this $\log-\log$ correlation. If there is a Gaussian distribution of intrinsic scatter in the SMBH mass at any fixed $\log n$, with a standard deviation which is independent of $\log n$ and equal to Δ , then the SMBH mass density should be increased by the factor $\exp[(\Delta \ln 10)^2/2]$ (Yu & Tremaine 2002, their equation 12). Such a Gaussian distribution, however, is not true for the scatter of points about the log-quadratic $M_{\text{bh}}-n$ relation shown in Fig.1; the scatter is clearly greater at the high-mass end. In fact, removal of the two highest mass SMBHs results in a log-quadratic relation consistent with zero intrinsic scatter (Graham & Driver 2007a). It is thus questionable whether one should apply this multiplicative term and because of this uncertainty, in what follows, we have not. However, one should note that if there were in fact no measurement errors and $\Delta = 0.31$ dex (the total absolute scatter about the $\log M_{\text{bh}}-\log n$ relation in Fig.1), then the corrective factor to apply to $\rho_{\text{bh},0}$ would be 1.29. If $\Delta = 0.18$ dex (the intrinsic scatter after factoring in the suspected measurement errors), then the multiplicative factor drops to 1.09. If there is no intrinsic scatter, then the multiplicative factor is simply 1.

3.2.3 SMBH baryon fraction

The above numbers can be expressed in terms of the baryon fraction of the universe. Already a picture is emerging in which dark accretion onto SMBHs may be negligible. Shankar et al. (2004) claim that the local SMBH mass function can be accounted for from mass accreted by X-ray se-

¹¹ For $H_0 = 70 \text{ km s}^{-1} \text{ Mpc}^{-1}$, $\rho_{\text{crit}} \sim 1.36 \times 10^{11} M_\odot \text{ Mpc}^{-3}$.

Table 3. Best-fitting parameters from the empirical SMBH mass function given in equation 2. The number density, ϕ_* , is per decade in SMBH mass. The late-type galaxy sample is not shown here due to the poor match between the empirical model and the data (see Fig.6). Sample 2 excludes bulges in disc galaxies if the core colour is bluer than $(u-r)_c = 2.00$ mag. Sample 3 (our primary sample) excludes blue bulges and blue elliptical galaxies if $(u-r)_c \leq 2.00$ mag (see Section 5.2).

Data sample	h_{70}^3	$\log \phi_*$ Mpc $^{-3}$ dex $^{-1}$	$\log(M_*/M_\odot)$	α
Early- and Late-type, ($B/T > 0.01$):				
Sample 1: no colour cut		-2.76	8.45	-0.32
Sample 2: $(u-r)_c$ [bulges] > 2.00 mag		-2.76	8.43	-0.29
Sample 3: $(u-r)_c$ [all] > 2.00 mag		-2.81	8.46	-0.30
Early-type, ($B/T > 0.4$):				
Sample 1: no colour cut		-2.68	8.26	0.07
Sample 2: $(u-r)_c$ [bulges] > 2.00 mag		-2.67	8.25	0.10
Sample 3: $(u-r)_c$ [all] > 2.00 mag		-2.74	8.29	0.00

lected AGN, i.e. no significant ‘dark’ accretion is required for SMBH growth (see also Cao 2007). If correct, this would imply that the growth of SMBHs from the accretion of massive black hole remnants of Population III stars may be small (Madau & Rees 2001; Islam, Taylor & Joseph 2003; Wyithe & Loeb 2004). Moreover, baryonic-fuelling is consistent with a picture that links the BH mass to the host spheroid’s baryonic, or at least stellar, properties, such as luminosity (e.g., Erwin, Graham & Caon 2002; McLure & Dunlop 2002; Marconi & Hunt 2003 and references therein), concentration (Graham et al. 2001; Graham & Driver 2007a) and mass (Magorrian et al. 1998; Häring & Rix 2004). Assuming the above standard picture in which SMBHs form via the accretion of baryons (Blandford 2004), then in terms of the invariant baryon fraction of the total mass-energy density, such that $\Omega_{\text{baryon}} = 0.0453h_{70}^{-2}$ (Tegmark et al. 2006, their Table 2, row 3; see also Blake et al. 2007), *SMBHs at the centres of galaxies today contain* $(0.007 \pm 0.003)h_{70}^3$ per cent of the universe’s baryon inventory.

Letting M_{spheroid} denote the stellar mass of a spheroid, Häring & Rix (2004) have shown that $M_{\text{bh}}/M_{\text{spheroid}} = 0.0009$ when $M_{\text{bh}} = 10^6 M_\odot$ and $= 0.0019$ when $M_{\text{bh}} = 10^9 M_\odot$, confirming the results given in Merritt & Ferrarese (2001, their Section 3; see also Laor 2001). Taking the average (or using the peak in our SMBH mass function at $\log(M_{\text{bh}}) = 8.3$, see Fig.6) one obtains M_{bh} equals 0.14 per cent of M_{spheroid} (or 0.16 per cent). Dividing $\Omega_{\text{bh}}/\Omega_{\text{baryon}}$ by this value one obtains $\Omega_{\text{spheroid}} \sim 6$ per cent (or ~ 5 per cent) of Ω_{baryon} . This is of course just a rough estimate, and a more precise value obtained using the actual spheroid luminosity function will be presented in Driver et al. (2007a, 2007b).

3.2.4 Comments on the low mass end

Figure 7 shows how the SMBH space density is built up as one includes (intrinsically) fainter spheroids, for our three galaxy bins. As was noted in Section 2, we excluded spheroids fainter than $M_B = -18$ mag in our analysis. For the early-type galaxy sample, Figure 7 reveals that integrating down to an absolute magnitude of -16 B-mag gives a SMBH mass density that is consistent (at the 2- σ level) with the result obtained using only those spheroids brighter than -18 B-mag. We do however caution that the SMBH masses

are less reliable in this regime, and as such we do not wish to place too much emphasis on this result.

It is also worth noting that the central massive object in spheroids fainter than $M_B \sim -18$ mag is often a nuclear star cluster (Ferrarese et al. 2006, left panel of their figure 2; Balcells et al. 2007). It is therefore questionable as to whether or not one should include such faint spheroids in an analysis of this kind. Moreover, if they are not individually modelled, the presence of additional nuclear star clusters can bias the Sérsic $R^{1/n}$ fit to give spuriously high values of the index n . The effect is to over-estimate the contribution from SMBHs in faint spheroids. Given the high frequency of nucleated bulges in spiral galaxies (e.g., Carollo, Stiavelli, & Mack 1998; Balcells et al. 2003), there is thus reason to doubt the rising SMBH space density curve shown in Fig.7 for the late-type galaxies.

4 COMPARISON WITH PAST ESTIMATES

McLure & Dunlop (2004) provided two estimates of the SMBH mass function (in early-type galaxies) using two techniques. At the low-mass end ($< 10^8 M_\odot$) their estimates do not agree; the mass function they obtained using the $M_{\text{bh}}-L$ relation gave noticeably higher SMBH number densities than they obtained using the $M_{\text{bh}}-\sigma$ relation (Fig.8, lower panel). Both the method and data that we have used is different to that used in McLure & Dunlop (2004) and thus provides an independent check on the SMBH mass function. Our analysis, using the $M_{\text{bh}}-n$ relation, shows a mass function which declines with decreasing SMBH masses that are less than $10^8 M_\odot$, and therefore better matches McLure & Dunlop’s mass function constructed using the $M_{\text{bh}}-\sigma$ relation rather than the $M_{\text{bh}}-L$ relation.

In plotting the mass functions from McLure & Dunlop (2004) in Fig.8, we have multiplied their ($M_{\text{bh}}-L$)-derived masses by 1.70. This increase stems from the conversion of their R-band $M_{\text{bh}}-L$ relation to the K-band. Starting from

equation 6 in McLure & Dunlop (2002)¹², one has

$$\begin{aligned} \log(M_{\text{bh}}/M_{\odot}) &= -0.5M_R - 2.91 \\ &= -0.5[M_K + 2.7 - M_{K,\odot} + 3.28 - 5 \log(70/50)] - 2.91 \\ &= 1.25 \log(L_K/L_{K,\odot}) - 5.53 \quad (9) \end{aligned}$$

Following McLure & Dunlop (2002), we have assumed an average $R-K$ colour of 2.7. We have used $M_{K,\odot} = 3.28$ mag (Binney & Merrifield 1998). McLure & Dunlop (2002) used the SMBH masses derived using Tonry et al.’s (2001) surface brightness fluctuation distances — which are independent of the Hubble constant. However they did not use these h -independent distances in deriving the absolute magnitude of the bulges, but used redshift derived distances and $H_0 = 50$ km s⁻¹ Mpc⁻¹. Equation 9 gives SMBH masses that are 0.23 dex larger than equation 1 in McLure & Dunlop (2004), and hence the factor of 1.70 (see Graham & Driver 2007b for more details).

In the lower panel of Fig.8, one can see that our analysis suggests there may be a greater (up to a factor of ~ 2) number density of SMBHs with masses $\log(M_{\text{bh}}/M_{\odot}) \sim 8.5$ than reported in McLure & Dunlop (2004). At smaller masses, $8 > \log(M_{\text{bh}}/M_{\odot}) > 6$, our mass functions roughly display the same decline with decreasing SMBH mass as McLure & Dunlop’s analysis based on the $M_{\text{bh}}-\sigma$ relation. Such a declining SMBH mass function (for early-type galaxies) is also in qualitative agreement with Shankar et al.’s (2004) mass function derived using a bivariate velocity dispersion distribution. In passing we note that we have increased Shankar et al.’s SMBH masses by 14 per cent, after adjusting for the correct dependence on the Hubble constant (see Graham & Driver 2007b). On the other hand, our data disagree with mass functions that rise monotonically (which includes asymptotically) towards lower-mass SMBHs, such as the ($M_{\text{bh}}-L$)-derived mass functions in McLure & Dunlop (2002), Aller & Richstone (2002) and Shankar et al. (2004).

The upper panel of Fig.8 reveals a clear disagreement, at masses below $\sim 10^8 M_{\odot}$, between our (total) mass function and that derived from $M_{\text{bh}}-L$ relations. We are not aware of any ($M_{\text{bh}}-\sigma$)-derived mass function for late-type galaxies, and therefore we do not show any such curve in this panel. Some of the mismatch from the ($M_{\text{bh}}-L$)-derived SMBH masses may stem from the methods used to assign bulge flux in lenticular and spiral galaxies (see Graham & Driver 2007b and Graham 2007).

Over the past few years a number of papers have constructed the local SMBH mass function and estimated the local SMBH mass density, $\rho_{\text{bh},0}$. We have listed several of these in Table 4. It can be seen that our estimates of $\rho_{\text{bh},0}$ agree particularly well with the estimate in Fukugita & Peebles (2004), and is consistent (within the $1-\sigma$ error bounds) with several other recent studies. It is worth noting, however, that our estimates are a factor of ~ 2 greater than reported in Wyithe (2006) and Aller & Richstone (2002). Due to the declining number density with decreasing SMBH mass, our

adopted integration across the complete mass spectrum of SMBHs, rather than truncating at $10^6 M_{\odot}$, does not significantly increase our estimate of $\rho_{\text{bh},0}$.

In an effort to try and understand why our SMBH mass densities may be slightly higher than reported by some, Graham & Driver (2007b) has examined two representative studies; one which used the $M_{\text{bh}}-\sigma$ relation (Aller & Richstone 2002) and the other the $M_{\text{bh}}-L$ relation (Shankar et al. 2004). Graham & Driver identified a number of corrections which can be made and showed that the mass density from Aller & Richstone (2002) is more than a factor of ~ 2 too low. As with the analysis by McLure & Dunlop, which was a factor of 1.7 too low, the reason is because of over-looked dependencies on the Hubble constant. These have been corrected in Figure 8, but not incorporated into Table 4.

5 POTENTIAL BIASES IN OUR DATA

5.1 A Linear $M_{\text{bh}}-n$ relation

While we believe the quadratic relation between M_{bh} and n (equation 1) is the optimal expression to use when predicting M_{bh} from n , we have explored how $\rho_{\text{bh},0}$ would change if we adopted the linear relation presented in Graham & Driver (2007a, their equation 2). Although a linear fit to the data in Figure 1 results in predictions of larger SMBH masses at the high- n end, over the range $\sim 2 < n < \sim 8$ it actually predicts lower SMBH masses (see Figure 3 in Graham & Driver 2007a). Because the bulk of the MGC data falls in this interval (see Figure 3)¹³, use of the linear $M_{\text{bh}}-n$ relation results in a 34 per cent lower SMBH mass density. This value is consistent, i.e. within the $1-\sigma$ uncertainty, with our estimate $\rho_{\text{bh},0} = (4.4 \pm 1.7) \times 10^5 h_{70}^3 M_{\odot} \text{ Mpc}^{-3}$. However, as noted in Graham & Driver (2007a), this linear relation has an intrinsic scatter of 0.31 dex, and so the estimate of $\rho_{\text{bh},0}$ should be increased by 29 per cent, to give a value of $3.8 \times 10^5 h_{70}^3 M_{\odot} \text{ Mpc}^{-3}$.

We have additionally removed the three high- n data points from Figure 1 and obtained a new linear relation with the remaining 24 data points. Doing so results in a relation with zero intrinsic scatter and a mass density that is 43 per cent higher than obtained with the quadratic relation. Specifically, we obtain a value of $(6.3 \pm 2.5) \times 10^5 h_{70}^3 M_{\odot} \text{ Mpc}^{-3}$, which is only marginally higher than our upper $1-\sigma$ value of $6.1 \times 10^5 h_{70}^3 M_{\odot} \text{ Mpc}^{-3}$. We also find $\rho_{\text{bh,early-type}} = (4.0 \pm 1.2) \times 10^5 h_{70}^3 M_{\odot} \text{ Mpc}^{-3}$ and $\rho_{\text{bh,late-type}} = (2.3 \pm 1.3) \times 10^5 h_{70}^3 M_{\odot} \text{ Mpc}^{-3}$.

The associated SMBH mass functions are shown in Figure 9 and given in Table 5. We caution that we do not believe

¹² Transformation of equation 5 in McLure & Dunlop (2002) would be considerably more difficult because it was constructed from an inactive plus active galaxy sample, a fraction of which have distances that depend on the Hubble constant and also on the adopted cosmology given that some of the active galaxies have redshifts which extend out to ~ 0.5 .

¹³ We *speculate* that the apparent shortage of Sérsic indices greater than ~ 8 in the MGC data (compared to Figure 1) may arise from GIM2D’s difficulty in deriving such large values while producing a galaxy magnitude that is close to the value obtained using SExtractor (due to the large wings of high- n profiles). Confirmation of this speculation would require simulations beyond the scope of this paper. We therefore offer it as nothing more than speculation, but do note that if correct, a variety of plausible stretches to the MGC values of n that we tested (to recover the possible true distribution) resulted in a ~ 20 per cent increase to the value of $\rho_{\text{bh},0}$ (i.e., smaller than our current $1-\sigma$ uncertainties on this value).

Table 4. Local SMBH mass density estimates. The difference between Samples 1 and 3 (see Section 5.2) in our study is that the latter excludes galaxies with $(u - r)_{\text{core}} < 2.00$ mag, such as blue pseudo-bulges. The factor $h_{70}^3 = [H_0/(70 \text{ km s}^{-1} \text{ Mpc}^{-1})]^3$ is appropriate for our study because the $M_{\text{bh}}-n$ relation is independent of the Hubble constant. The majority of the densities from other papers have been transformed to $H_0 = 70 \text{ km s}^{-1} \text{ Mpc}^{-1}$ using h^2 rather than h^3 , as indicated in each paper. However, as discussed in Graham & Driver (2007b), this may not always be appropriate.

Study	$\rho_{\text{bh},0}$ (E/S0)	$\rho_{\text{bh},0}$ (Sp)	$\rho_{\text{bh},0}$ (total)
	$h_{70}^2 10^5 M_{\odot} \text{ Mpc}^{-3}$	$h_{70}^2 10^5 M_{\odot} \text{ Mpc}^{-3}$	$h_{70}^2 10^5 M_{\odot} \text{ Mpc}^{-3}$
This study (Sample 1)	$(3.8 \pm 1.3)h_{70}$	$(1.1 \pm 0.6)h_{70}$	$(4.9 \pm 1.9)h_{70}$
This study (Sample 3)	$(3.5 \pm 1.2)h_{70}$	$(1.0 \pm 0.5)h_{70}$	$(4.4 \pm 1.7)h_{70}$
Wyithe (2006)	2.28 ± 0.44
Fukugita & Peebles (2004) ^a	$(3.4^{+3.4}_{-1.7})h_{70}^{-1}$	$(1.7^{+1.7}_{-0.8})h_{70}^{-1}$	$(5.1^{+3.8}_{-1.9})h_{70}^{-1}$
Marconi et al. (2004)	3.3	1.3	$4.6^{+1.9}_{-1.4}$
Shankar et al. (2004) ^b	$3.1^{+0.9}_{-0.8}$	$1.1^{+0.5}_{-0.5}$	$4.2^{+1.1}_{-1.1}$
McLure & Dunlop (2004)	2.8 ± 0.4
Wyithe & Loeb (2003)	$2.2^{+3.9}_{-1.4}$
Aller & Richstone (2002) ^c	1.8 ± 0.6	0.6 ± 0.5	2.4 ± 0.8
Yu & Tremaine (2002) ^d	2.0 ± 0.2	0.9 ± 0.2	2.9 ± 0.4
Merritt & Ferrarese (2001) ^e	$4.6h_{70}^{-1}$
Salucci et al. (1999)	6.2	2.0	8.2

^a See their equation 75.

^b Based on their $(M_{\text{bh}}-L)$ -derived mass function, and in agreement with their $(M_{\text{bh}}-\sigma)$ -derived values.

^c Taken from their Table 2.

^d Based on their $(M_{\text{bh}}-\sigma)$ -derived mass function.

^e See also Ferrarese (2002).

these are more accurate than those provided in Table 1, but that they provide an (extreme) upper limit to the SMBH mass function and space density. As was noted in Section 2, the evidence for a curved $M_{\text{bh}}-n$ relation is inherent in the low- n data. Excluding the five highest n galaxies results in a quadratic relation that is fully consistent with equation 1. Removing the two galaxies with the highest SMBH masses (one of which is suspected to be biased high: NGC 4486) produces the same result. The linear relation obtained after removing the three high n galaxies is thus entirely driven by two galaxies (NGC 4486 and NGC 4649).

5.2 Blue Spheroids and Pseudobulges

We divided each of the early-type (E/S0), late-type (Sp) and (early + late)-type galaxy bins into three (colour) samples. Sample 1 has had no modifications to it, while Sample 2 excludes bulges (in disc galaxies) if the $(u - r)$ core colour is bluer than 2.00 mag. The core-colour is derived from Sloan Digital Sky Survey point-spread-function magnitudes which have been shown to maximise the colour bimodality, see Driver et al. (2006a). This colour-cut may help avoid possible pseudo-bulges (e.g., Erwin et al. 2003; Kormendy & Kennicutt 2004; Kormendy & Fisher 2005) which may or may not have SMBHs. Sample 3 is further reduced to exclude all systems (i.e., bulges and elliptical galaxies) with $(u - r)_c < 2.00$ mag (see Fig.10).

It is not clear whether supermassive black holes exist in (every) pseudo-bulge. The tight correlation between the properties of dynamically hot spheroids and their black hole mass has been tied to their joint formation process. As pseudo-bulges are believed to have formed via a distinctly

Table 5. Supermassive black hole mass function data (corrected for Malmquist bias) for the full, early- and late-type galaxy sample (Sample 3, see Section 5.2) shown in Figure 9. The linear $M_{\text{bh}}-n$ relation (Section 5.1), obtained after excluding the three galaxies with the highest Sérsic index, has been used here to provide an upper estimate to the SMBH mass function. The uncertainties given are the upper and lower quartiles (i.e. ± 25 per cent) from extensive Monte Carlo realisation of the combined errors.

$\log_{10} M_{\text{bh}}$ M_{\odot}	$\phi(10^{-4} h_{70}^3 \text{ Mpc}^{-3} \text{ dex}^{-1})$		
	All galaxies	Early-type	Late-type
5.00	$0.12^{+0.12}_{-0.07}$	$0.06^{+0.04}_{-0.04}$	$0.08^{+0.12}_{-0.08}$
5.25	$0.00^{+0.16}_{-0.00}$	$0.00^{+0.07}_{-0.00}$	$0.00^{+0.15}_{-0.00}$
5.50	$1.13^{+0.17}_{-0.16}$	$0.00^{+0.08}_{-0.00}$	$1.26^{+0.14}_{-0.13}$
5.75	$0.84^{+0.17}_{-0.15}$	$0.42^{+0.10}_{-0.09}$	$0.44^{+0.14}_{-0.13}$
6.00	$0.00^{+0.19}_{-0.00}$	$0.00^{+0.13}_{-0.00}$	$0.11^{+0.14}_{-0.13}$
6.25	$1.28^{+0.23}_{-0.21}$	$0.45^{+0.18}_{-0.15}$	$0.84^{+0.15}_{-0.14}$
6.50	$0.00^{+0.39}_{-0.00}$	$0.00^{+0.42}_{-0.00}$	$0.00^{+0.15}_{-0.00}$
6.75	$4.33^{+0.67}_{-0.70}$	$2.96^{+0.64}_{-0.67}$	$1.34^{+0.15}_{-0.15}$
7.00	$4.68^{+0.58}_{-0.57}$	$4.48^{+0.57}_{-0.59}$	$0.19^{+0.17}_{-0.16}$
7.25	$8.76^{+0.61}_{-0.60}$	$8.22^{+0.55}_{-0.55}$	$0.54^{+0.18}_{-0.16}$
7.50	$8.37^{+0.75}_{-0.68}$	$7.21^{+0.69}_{-0.65}$	$1.13^{+0.18}_{-0.18}$
7.75	$13.20^{+0.96}_{-0.88}$	$12.03^{+0.87}_{-0.83}$	$1.17^{+0.19}_{-0.19}$
8.00	$16.23^{+1.14}_{-1.01}$	$15.88^{+1.01}_{-0.89}$	$0.35^{+0.23}_{-0.22}$
8.25	$13.93^{+0.96}_{-0.90}$	$11.85^{+0.87}_{-0.80}$	$2.11^{+0.32}_{-0.29}$
8.50	$12.89^{+0.93}_{-0.98}$	$9.52^{+0.90}_{-0.94}$	$3.39^{+0.27}_{-0.27}$
8.75	$5.45^{+1.11}_{-1.09}$	$4.48^{+0.89}_{-0.76}$	$1.05^{+0.32}_{-0.31}$
9.00	$3.69^{+0.57}_{-0.50}$	$2.51^{+0.48}_{-0.43}$	$1.18^{+0.17}_{-0.15}$
9.25	$1.50^{+0.41}_{-0.39}$	$1.50^{+0.33}_{-0.33}$	$0.00^{+0.14}_{-0.00}$
9.50	$0.94^{+0.29}_{-0.25}$	$0.42^{+0.27}_{-0.25}$	$0.52^{+0.10}_{-0.09}$

Note: number densities are scaled to per unit $\log M_{\text{bh}}$ interval and not per 0.25 $\log M_{\text{bh}}$ interval.

different formation process (i.e., from a redistribution of stars due to perpendicular-to-the-disc resonances with a bar) it is plausible that pseudo-bulges do not possess SMBHs. Despite this conjecture, we note that bars can fuel AGN growth (e.g., Ann & Thakur 2005; Combes 2006; Ohta et al. 2006). Moreover, the Milky Way has a SMBH mass that appears consistent with both the $M_{\text{bh}}-n$ and $M_{\text{bh}}-\sigma$ relations and probably has a pseudo-bulge — suggested from its rotation (e.g., Minniti et al. 1992), flattening (e.g., Sharples, Walker & Cropper 1990; Lopez-Corredoira et al. 2005), presence of a bar (e.g., Lopez-Corredoira et al. 2006) and peanut-shaped structure (e.g., Alard 2001, see also Debattista et al. 2006), but see Zoccali et al. (2006) and Matteucci (2006). The situation is therefore ambiguous, which has resulted in our decision to create three subsamples.

To unequivocally distinguish dynamically hot bulges from rotating pseudo-bulges requires kinematical information. In the absence of this, an effective method is to use colour, with the pseudo-bulges typically exhibiting blue colours comparable to a young (metal rich) disc population and the genuine bulges exhibiting red colours consistent with an old population. We do however note that in some cases the bulges are poorly resolved and the central colour is thus a blend of the bulge and disc, which might result in some real bulges erroneously falling blueward of our colour cut. However the fact that the colour bimodality is clearly evident in our data suggests this is probably not a major issue, and we note that a positive correlation between bulge and disc colour is known to exist (e.g., Peletier & Balcells 1996).

Including blue spheroids with $(u-r)_c < 2.00$ mag, Sample 1 gives densities of $\rho_{\text{bh,early-type}} = (3.8 \pm 1.3) \times 10^5 h_{70}^3 M_{\odot} \text{Mpc}^{-3}$ and $\rho_{\text{bh,late-type}} = (1.1 \pm 0.6) \times 10^5 h_{70}^3 M_{\odot} \text{Mpc}^{-3}$ (Table 2).

6 SUMMARY

We have used the log-quadratic relation between supermassive black hole mass and the host spheroid's Sérsic index n (i.e. the $M_{\text{bh}}-n$ relation, Graham & Driver 2007a) to predict the SMBH masses in galaxies from the Millennium Galaxy Catalogue (MGC) for which a two-dimensional, seeing-corrected, $R^{1/n}$ -bulge plus exponential-disc decomposition has been performed (Allen et al. 2006).

Applying the appropriate volume corrections, the number density of SMBHs with masses greater than $10^6 M_{\odot}$, and in spheroids more luminous than $M_B = -18$ mag, is $(2.3 \pm 0.1) \times 10^{-3} h_{70}^3 \text{Mpc}^{-3}$.

We have constructed the local ($0.013 < z < 0.18$, $\bar{z} = 0.12$) SMBH mass function using direct estimates of the M_{bh} predictor-quantity n (Fig.6). Using every spheroid, the SMBH mass function appears well represented by a 3-parameter Schechter function having a logarithmic slope at the low-mass end of around two-thirds. Excluding the late-type galaxies, identified as systems with bulge-to-total ratios smaller than 0.4, the SMBH mass function was again well fit with a Schechter function, this time having a low-mass slope of 1, and a turnover mass at $\sim 2 \times 10^8 M_{\odot}$.

Integrating down to a SMBH mass of $10^6 M_{\odot}$, the local mass density of SMBHs from early- and late-type galaxies combined is $\rho_{\text{bh},0} = (4.4 \pm 1.7) \times 10^5 h_{70}^3 M_{\odot} \text{Mpc}^{-3}$. This value is slightly greater than, but still consistent with, most

values obtained via independent means over recent years (Table 4, but see Graham & Driver 2007b). Our mass density estimate can be split into $\rho_{\text{bh,early-type}} = (3.5 \pm 1.2) \times 10^5 h_{70}^3 M_{\odot} \text{Mpc}^{-3}$ and $\rho_{\text{bh,late-type}} = (1.0 \pm 0.5) \times 10^5 h_{70}^3 M_{\odot} \text{Mpc}^{-3}$, based upon a B/T flux ratio cut at 0.4.

In terms of the critical density of the universe, we obtain $\Omega_{\text{bh,total}} = (3.2 \pm 1.2) \times 10^{-6} h_{70}$, or $\Omega_{\text{bh,early-type}} = (2.5 \pm 0.9) \times 10^{-6} h_{70}$ and $\Omega_{\text{bh,late-type}} = (0.7 \pm 0.4) \times 10^{-6} h_{70}$. Given that $4.5 h_{70}^{-2}$ per cent of the critical density is in the form of baryons (Tegmark et al. 2006), the above figures imply $(0.007 \pm 0.003) h_{70}^3$ per cent of the total baryon content of the universe is locked up in SMBHs at the centres of galaxies.

7 ACKNOWLEDGMENTS

A.G. would like to thank St Andrews University's School of Physics & Astronomy for its hospitality during a 3 week visit to work on this paper. We are happy to thank Francesco Shankar for kindly supplying us with the data from his ($M_{\text{bh}}-\sigma$)-derived SMBH mass function shown in Shankar et al. (2004, their Fig.7). We are additionally grateful to Francoise Combes for her helpful comments about the Milky Way. The Millennium Galaxy Catalogue consists of imaging data from the Isaac Newton Telescope at the Spanish Observatorio del Roque de Los Muchachos of the Instituto de Astrofísica de Canarias, and spectroscopic data from the Anglo Australian Telescope, the ANU 2.3 m, the ESO New Technology Telescope, the Telescopio Nazionale Galileo, and the Gemini Telescope. This research has made use of the NASA/IPAC Extragalactic Database (NED) which is operated by the Jet Propulsion Laboratory, California Institute of Technology, under contract with the National Aeronautics and Space Administration. The survey has been supported through grants from the United Kingdom Particle Physics and Astronomy Research Council, and the Australian Research Council through Discovery Project Grant DP0451426. The data and data products are publicly available from <http://www.eso.org/~jlliske/mgc/> or on request from J. Liske or S.P. Driver.

REFERENCES

- Adelman-McCarthy, J.K., et al. 2007, ApJS, submitted
- Alard, C., 2001, A&A, 379, L44
- Allen, P., Driver, S.P., Graham, A.W., Cameron, E., Liske, J., De Propriis, R., 2006, MNRAS, in press (astro-ph/0605699)
- Aller, M.C., Richstone, D., 2002, AJ, 124, 3035
- Andredakis, Y.C., Peletier, R.F., Balcells, M., 1995, MNRAS, 275, 874
- Andredakis, Y.C., Sanders, R.H., 1994, MNRAS, 267, 283
- Ann, H.B., & Thakur, P., 2005, ApJ, 620, 197
- Balcells, M., Graham, A.W., Dominguez-Palmero, L., Peletier, R.F., 2003, ApJ, 582, L79
- Balcells, M., Graham, A.W., Peletier, R.F., 2007, ApJ, submitted (astro-ph/0404381)
- Binney, J., Merrifield, M., 1998, Galactic astronomy, Princeton University Press, p.53
- Blake, C., Collister, A., Bridle, S., Lahav, O., 2007, MNRAS, 374, 1527
- Blandford, R.D. 2004, in "Carnegie Observatories Astrophysics

- Series, Vol.1: Coevolution of Black Holes and Galaxies," ed. L.C. Ho (Pasadena: Carnegie Observatories), p.153
- Blanton, M., et al., 2005, *AJ*, 129, 2562
- Blanton, M., Roweis, S., 2007, *AJ*, 133, 734
- Cao, X., 2007, *ApJ*, in press (astro-ph/0701007)
- Caon, N., Capaccioli, M., D'Onofrio, M., 1993, *MNRAS*, 265, 1013
- Carollo, C.M., Stiavelli, M., & Mack, J. 1998, *AJ*, 116, 68
- Combes, F., 2006, *Combes, F.* 2006, *IAU Symposium*, 235
- Debattista, V.P., Mayer, L., Carollo, C.M., Moore, B., Wadsley, J., Quinn, T., 2006, *ApJ*, 645, 209
- De Francesco, G., Capetti, A., Marconi, A., 2007, *A&A*, in press (astro-ph/0609603)
- de Jong, R.S., 1996, *A&AS*, 118, 557
- D'Onofrio, M., Capaccioli, M., & Caon, N. 1994, *MNRAS*, 271, 523
- D'Onofrio, M., 2001, *MNRAS*, 326, 1517
- Driver, S.P., Liske, J., Cross, N.J.G., De Propriis, R., Allen, P.D., 2005, *MNRAS*, 360, 81
- Driver, S.P., Allen, P.D., Graham, A.W., Cameron, E., Liske, J., Ellis, S.C., Cross, N.J.G., De Propriis, R., Phillips, S., Couch, W.J., 2006a, *MNRAS*, 368, 414
- Driver, S.P., Graham, A.W., Allen, P.D., Liske, J., 2006b, in *The Fabulous Destiny of Galaxies* (astro-ph/0509704)
- Driver, S.P., Liske, J., Graham, A.W., Allen, P.D., 2006c, *IAU Symposium*, 235, #4
- Driver, S.P., Allen, P.D., Liske, J., Graham, A.W., 2007a, *ApJ*, submitted
- Driver, S.P., Popescu, C.C., Tuffs, R.J., Liske, J., Graham, A.W., Allen, P.D., DePropriis, R., 2007b, *MNRAS*, submitted
- Efstathiou, G., Ellis, R.S., Peterson, B.A., 1988, *MNRAS*, 232, 431
- Erwin, P., Graham, A., Caon, N., 2002, in "Carnegie Observatories Astrophysics Series, Vol.1: Coevolution of Black Holes and Galaxies," ed. L.C. Ho (Pasadena: Carnegie Observatories) (astro-ph/0212335)
- Erwin, P., Vega Beltran, J.C., Graham, A.W., Beckman, J.E., 2003, *ApJ*, 597, 929
- Ferrarese, L., 2002, in *Proc. 2nd KIAS Astrophysics Workshop, Current High-Energy Emission around Black Holes*. Ed. C.-H.Lee. World Scientific, Singapore, p.3 (astro-ph/0203047)
- Ferrarese, L., et al. 2006, *ApJ*, 644, L21
- Ferrarese, L., & Ford, H., 2005, *Space Science Reviews*, 116, 523
- Franceschini, A., Vercellone, S., Fabian, A.C. 1998, *MNRAS*, 297, 817
- Fukugita, M., Peebles, P.J.E., 2004, *ApJ*, 616, 643
- Graham, A.W., 2001, *AJ*, 121, 820
- Graham, A.W., 2003, *AJ*, 125, 3398
- Graham, A.W., 2007, *MNRAS*, submitted
- Graham, A.W., Driver, S.P., 2007a, *ApJ*, 655, 77
- Graham, A.W., Driver, S.P., 2007b, *MNRAS*, submitted
- Graham, A.W., Driver, S.P., 2005, *PASA*, 22(2), 118 (astro-ph/0503176)
- Graham, A.W., Erwin, P., Caon, N., Trujillo, I., 2001, *ApJ*, 563, L11
- Graham, A.W. Erwin, P., Caon, N., Trujillo, I., 2003, in *Galaxy Evolution: Theory and Observations*, *RevMexAA (SC)*, ed. V.Avila-Reese, C.Firmani, C.S.Frenk, C.Allen, vol. 17, 196-197
- Guhathakurta, P., et al., 2006, *Nature*, submitted (astro-ph/0502366)
- Häring, N., Rix, H.-W., 2004, *ApJ*, 604, L89
- Hubble, E. 1926, *ApJ*, 64, 321
- Hubble, E. 1936, in *The Realm of the Nebulae* (Yale University Press, New Haven)
- Islam, R.R., Taylor, J.E., Silk, J., 2003, *MNRAS*, 340, 647
- Kaspi, S., Brandt, W.N., Maoz, D., Netzer, H., Schneider, D.S., Shemmer, O., *ApJ*, in press (astro-ph/0612722)
- Kent, S. 1985, *ApJS*, 59, 115
- Kormendy, J., 1993, in *The Nearest Active Galaxies*, ed. J.E.Beckman, L.Colina, & H.Netzer (Madrid: CSIC), 197
- Kormendy, J., & Fisher, D.B. 2005, *Revista Mexicana de Astronomia y Astrofisica Conference Series*, 23, 101
- Kormendy, J., Kennicutt, R.C.Jr., 2004, *ARA&A*, 42, 603
- La Barbera, F., de Carvalho, R.R., Gal, R.R., Busarello, G., Merluzzi, P., Capaccioli, M., Djorgovski, S.G., 2005, *ApJ*, 626, L19
- Laor, A. 2001, *ApJ*, 553, 677
- Ledlow, M.J., Owen, F.N., 1995, *AJ*, 110, 1959
- Liske, J., Lemon, D.J., Driver, S.P., Cross, N.J.G., Couch, W.J., 2003, *MNRAS*, 344, 307
- Liske, J., Driver, S.P., Allen, P.D., Cross, N.J.G., De Propriis, R. 2006, *MNRAS*, 369, 1547
- López-Corredoira, M., Cabrera-Lavers, A., Gerhard, O.E., 2005, *A&A*, 439, 107
- López-Corredoira, M., Cabrera-Lavers, A., Mahoney, T.J., Hammersley, P.L., Garzon, F., Gonzalez-Fernandez, C., 2006, *AJ*, in press
- MacArthur, L.A., Courteau, S., Holtzman, J.A., 2003, *ApJ*, 582, 689
- Madau, P., Rees, M.J., 2001, *ApJ*, 551, L27
- Madgwick, D.S., et al. 2002, *MNRAS*, 333, 133
- Magorrian, J., et al., 1998, *AJ*, 115, 2285
- Marconi, A., Hunt, L.K., 2003, *ApJ*, 589, L21
- Marconi, A., Risaliti, G., Gilli, R., Hunt, L.K., Maiolino, R., Salvati, M., 2004, *MNRAS*, 351, 169
- Marleau, F.R., Simard, L., 1998, *ApJ*, 507, 585
- Marzke, R.O., Geller, M.J., Huchra, J.P., & Corwin, H.G., 1994, *AJ*, 108, 437
- Matteucci, F., 2006, in *The Metal Rich Universe* (astro-ph/0610832)
- McLure, R.J., Dunlop, J.S., 2002, *MNRAS*, 331, 795
- McLure, R.J., Dunlop, J.S., 2004, *MNRAS*, 352, 1390 (MD04)
- Merritt, D., Ferrarese, L., 2001, *MNRAS*, 320, L30
- Minniti, D., White, S.D.M., Olszewski, E.W., Hill, J.M., 1992, *ApJ*, 393, L47
- Novak, G.S., Faber, S.M., Dekel, A., 2006, *ApJ*, 637, 96
- Ohta, K., Aoki, K., Kawaguchi, T., Kiuchi, G., 2006, *ApJ*, in press (astro-ph/0610355)
- Peletier, R.F., Balcells, M., 1996, *AJ*, 111, 2238
- Peletier, R.F., Davies, R.L., Illingworth, G.D., Davis, L.E., Cawson, M., 1990, *AJ*, 100, 1091
- Press, W.H., Teukolsky, S.A., Vetterling, W.T., & Flannery, B.P., 1992, *Numerical recipes* (2nd ed.; Cambridge: Cambridge Univ. Press)
- Ryan, C.J., De Robertis, M.M., Virani, S., Laor, A., Dawson, P.C., 2007, *ApJ*, 654, 799
- Salucci, P., Szuszkiewicz, E., Monaco, P., Danese, L., 1999, *MNRAS*, 307, 637
- Schechter, P. 1976, *ApJ*, 203, 297
- Shankar, F., Salucci, P., Granato, G.L., De Zotti, G., Danese, L., 2004, *MNRAS*, 354, 1020
- Sharples, R., Walker, A., Cropper, M. 1990, *MNRAS*, 246, 54
- Simard, L., et al., 2002, *ApJS*, 142, 1
- Simien, F., de Vaucouleurs, G., 1986, *ApJ*, 302, 564
- Taylor, V.A., Jansen, R.A., Windhorst, R.A., Odewahn, S.C., Hibbard, J.E., 2005, *ApJ*, 630, 784
- Tegmark, M., et al., 2006, *Phys.Rev.D.*, submitted (astro-ph/0608632)
- Tonry, J., et al., 2001, *ApJ*, 546, 681
- Trujillo, I., Graham, A.W., Caon, N., 2001, *MNRAS*, 326, 869
- Wyithe, J.S.B., 2006, *MNRAS*, 365, 1082
- Wyithe, J.S.B., Loeb, A., 2003, *ApJ*, 595, 614
- Wyithe, J.S.B., Loeb, A., 2004, *ApJ*, 612, 597
- Yu, Q., Tremaine, S., 2002, *MNRAS*, 335, 965
- Zoccali, M., et al. 2006, *A&A*, 457, L1

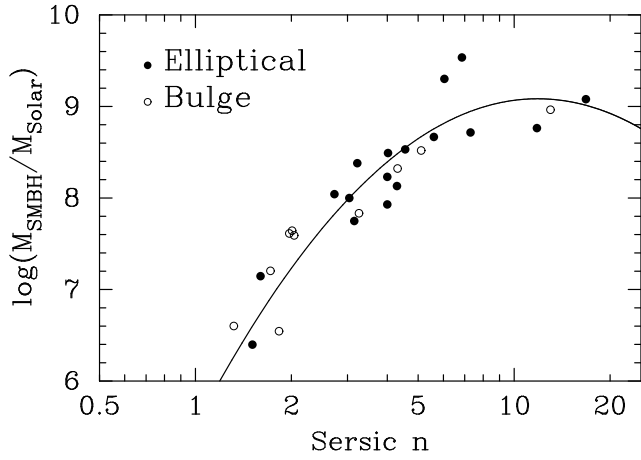


Figure 1. Relationship between SMBH mass and host spheroid Sérsic index. The data points were taken from Graham & Driver (2007a, their table 1) and the curve shows the best quadratic fit (equation 1).

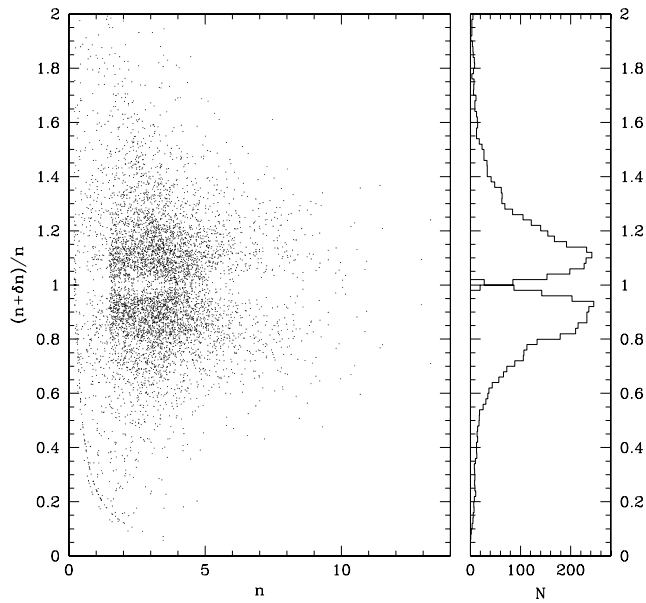


Figure 3. GIM2D-derived uncertainty in n , namely δn (which need not be symmetrical about n), is converted to a fractional uncertainty and shown as a function of n for the full MGC spheroid sample. Sixty eight per cent of the data has an error on n of less than 20 per cent. The bottom-left envelope of points in the left panel trace the lower limit on the value of n (equal to 0.2) that we set in GIM2D (see Allen et al. 2006). A second envelope arises from the 0.09 dex colour-correction which is applied to the bulges of the late-type galaxies (see Section 2.1).

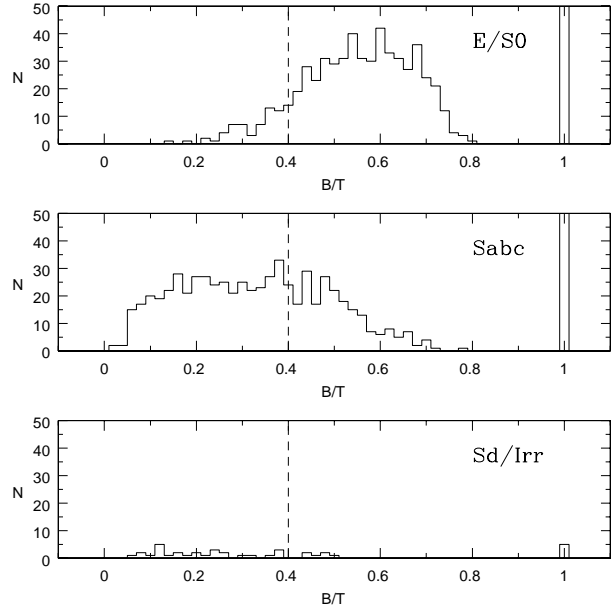


Figure 4. Distribution of GIM2D-derived, bulge-to-total flux ratios (B/T) for those MGC galaxies with an (eyeball) morphological classification (Driver et al. 2006a). Galaxies with a core colour bluer than $(u-r)_c = 2.00$ mag have been excluded from the top panel. Spheroids fainter than $M_B = -17$ mag and effective half-light radii smaller than 0.333 arcseconds (1 pixel) have been excluded from all panels. The dashed line at $B/T = 0.4$ denotes our adopted divide between early- and late-type galaxies.

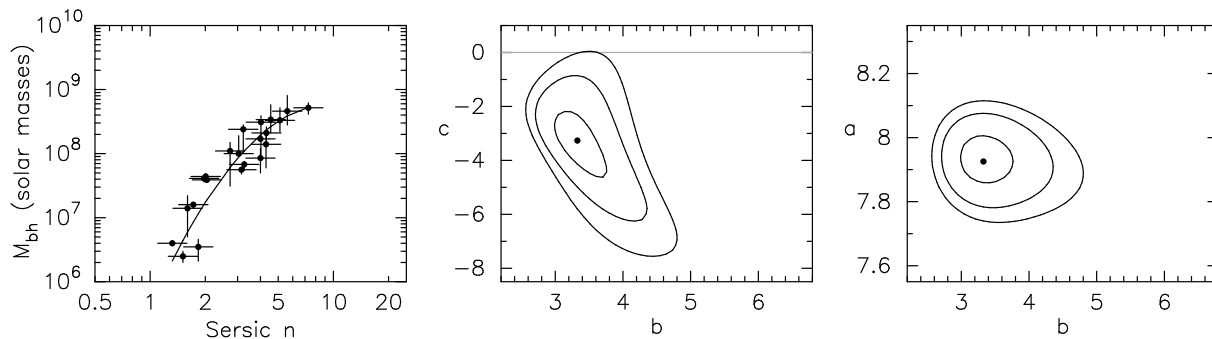


Figure 2. Left panel: Variant of Fig.1 after removing the five data points with the highest SMBH masses. The curved line corresponds to $\log M_{\text{bh}} = a + b \log(n/3) + c [\log(n/3)]^2$. Projections of the $\Delta\chi^2 = 1.00, 4.00$ and 6.63 contours, shown in the central and right panels, onto each axis gives the 68.3, 95.4, and 99 per cent confidence interval on each of the parameters a, b and c . The optimal log-quadratic relation (shown in the left panel) is consistent with zero intrinsic scatter and reveals that the coefficient, c , in front of the quadratic term is inconsistent with a value of zero at the $\sim 2.5 \sigma$ level. Subsequently, one can conclude that the log-quadratic relation in Eq.1 is not the result of increased scatter, i.e. outliers, at the high-mass end of the $M_{\text{bh}}-n$ relation (see Graham & Driver 2007a for more details).

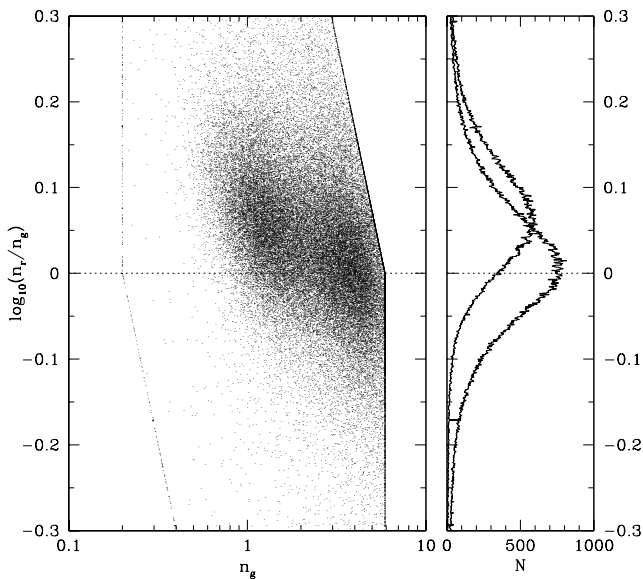


Figure 5. Logarithmic difference between the r - and g -band Sérsic indices from individual galaxies in the SDSS-VAGC (Blanton et al. 2005), in which a *single* $R^{1/n}$ function was fitted to each galaxy and the Sérsic index restricted to lie between 0.2 and 6. The peak of the distribution for galaxies with g -band Sérsic indices greater than 2.0 (i.e., predominantly bulge-dominated, early-type galaxies) is 0.003 dex. The peak of the distribution for galaxies with $n_g < 2.0$ (i.e., predominantly late-type galaxies) is 0.06 dex. The choice of $n_g = 2.0$ originates from the Sérsic index bimodality plots in Driver et al. (2006a). While the right-hand panel is based on all the SDSS-VAGC data, the left hand panel shows a random sample of 75,000 with $n_g > 2.0$ and 75,000 with $n_g < 2.0$. Such a restriction prevents washing away the structure in the left panel with too many data points.

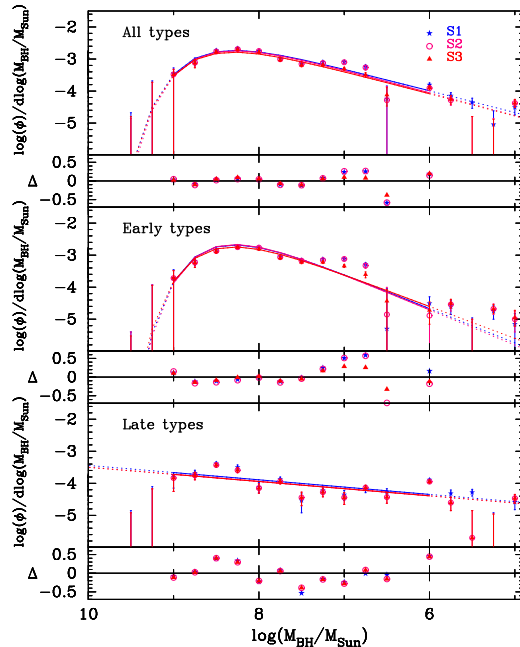


Figure 6. Black hole mass functions for our three (colour) samples, e.g. S3 = Sample 3, see Section 5.2. Early-type galaxies are those with $B/T > 0.4$ (see Fig.4). The best-fitting 3-parameter models (equation 2) are shown. Model parameters are given in Table 3. The number density shown along the vertical axis is expressed in units of $h_{70}^3 \text{ Mpc}^{-3}$ per decade in SMBH mass. The fitting is performed over the SMBH mass range $10^9 > M_{\text{bh}}/M_{\odot} > 10^6$. Residuals about the models are shown beneath each fit.

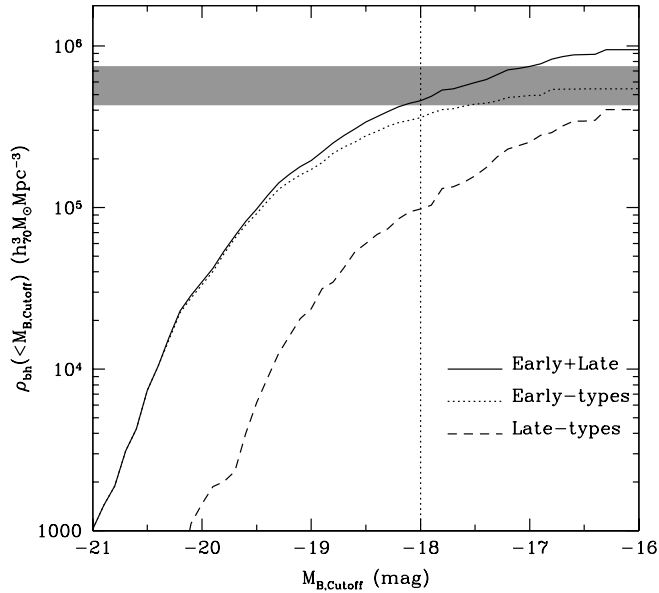


Figure 7. Cumulative SMBH space density, ρ_{bh} . Our early-type galaxies are those with $B/T > 0.4$, while our late-type galaxies have $0.01 < B/T \leq 0.4$. The cutoff at an absolute magnitude of -18 B-mag marks the boundary to which we can trust our data. The horizontal shading is centred on the (H_0 corrected, i.e. 41 per cent increased) solution for (early+late)-type galaxies by Shankar et al. (2004, their section 3.2), and shows their quoted $1\text{-}\sigma$ uncertainty.

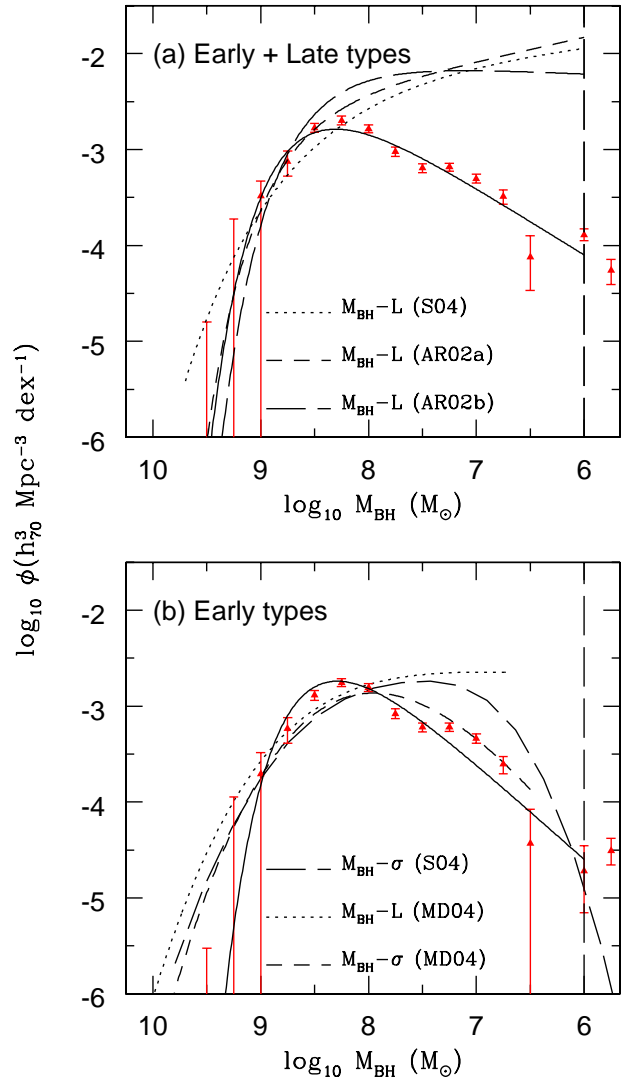


Figure 8. Our observed SMBH mass functions, along with our fits to Sample 3 (solid curves), overlaid with others estimates of the mass function. Shown in the top panel are curves from Shankar et al. (2004; S04) and Aller & Richstone (2002): (AR02)a is based on the Madgwick et al. (2002) luminosity function, and (AR02)b is based on the Marzke et al. (1994) luminosity function. Shown in the lower panel are curves from Shankar et al. (2004), and also McLure & Dunlop (2004; MD04) who used two independent techniques (see Section 4). The ($M_{\text{bh}}\text{-}\sigma$)-derived mass functions can be seen to turn down at low-masses, in agreement with our ($M_{\text{bh}}\text{-}n$)-derived mass function. We have corrected all curves to $H_0 = 70 \text{ km s}^{-1} \text{ Mpc}^{-1}$, following the prescription given by Graham & Driver (2007b).

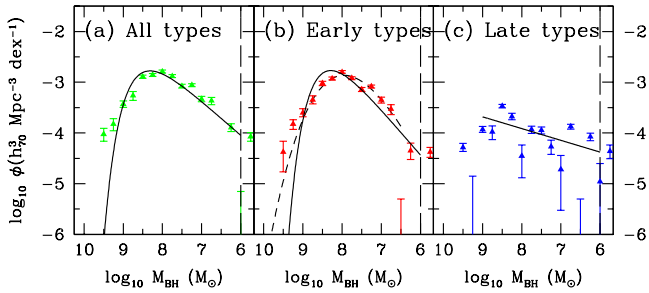


Figure 9. Our (extreme) high-mass SMBH mass function constructed using the linear $M_{\text{bh}}-n$ relation which excluded the three highest- n galaxies (see Section 5.1). The solid curves are the optimal fits shown in Figure 6. The dashed curve in the middle panel is the $(M_{\text{bh}}-L)$ -derived mass function given in McLure & Dunlop (2004).

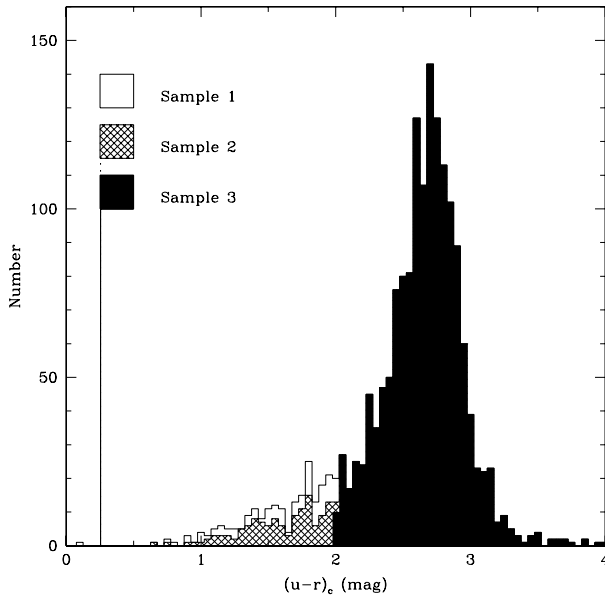


Figure 10. The $(u-r)_c$ core colour distribution of the three spheroid samples. Only galaxies with $B/T > 0.01$ and $M_B < -18$ mag are shown. A colour cut at $(u-r)_c = 2.00$ mag reflects the central minimum observed in the bimodal distribution of core colours shown in Liske et al. (2007, in prep.).